Structural, Spectroscopic, and Theoretical Study of Ferrocene Ureidopeptides

Jasmina Lapić,[†] Gordana Pavlović,[‡] Daniel Siebler,[§] Katja Heinze,*[,§] and Vladimir Rapić*[,†]

Department of Chemistry and Biochemistry, Faculty of Food Technology and Biotechnology, University of Zagreb, Pierottijeva 6, HR-10000 Zagreb, Croatia, Department of Applied Chemistry, Faculty of Textile Technology, University of Zagreb, Prilaz Baruna Filipovića 30, HR-10000 Zagreb, Croatia, and Department of Inorganic Chemistry, University of Heidelberg, Im Neuenheimer Feld 270, 69120 Heidelberg, Germany

Received September 25, 2007

Ferrocene ureidopeptides **3** and **4** and their derivatives **7** and **8** with a methyl ester substituent in 1′ position of the ferrocene have been prepared starting from ferrocenecarboxazide (**1**) or methyl 1′-azidocarbonylferrocene-1-carboxylate (**5**) via the corresponding isocyanatoferrocenes (**2/6**) and their coupling with alanine and alanylalanine methyl esters. Thorough spectroscopic and theoretical analyses revealed that in systems **4**, **7**, and **8** intramolecular hydrogen bonds play only a minor role, while self-assembly processes prevail in solution and in the solid state with urea NH groups acting as hydrogen donors and alanine amide and alanine ester CO groups acting as hydrogen acceptors. The ester substituent in the 1′ position of the ferrocene in compounds **7** and **8** does not engage in hydrogen bonding.

Introduction

(Oligo)urea peptidomimetics are formally derived from peptides by replacement of amido groups with urea moieties under addition of two methylene groups per repeating unit. These molecules offer several advantages in comparison with natural peptides regarding possible therapeutic applications.[1–5] On the other hand Nowick and North showed that urea-derived small molecules can act as molecular scaffolds for studies of protein folding. Generally, such molecular scaffolds constrain the attached peptide chains to adopt specific conformations; that is, they are α-, β-, or γ-turn inducers. Such peptidomimetics ("ureidopeptides") may derive from T = nornaboran-5-en-2,3-diyl, cyclopropane-1,2-diyl (Scheme 1, type **I**) and T = $-CH_2CH_2-$, R = $NCCH_2CH_2-$ (Scheme 1, type **II**), forming β-sheet-like structures with parallel peptide strands. CO and NH groups from both the peptide strands and the urea moieties can be involved in intramolecular hydrogen bonds (IHBs).[6–8]

Ferrocene-containing peptides and peptide analogues (peptidomimetics) play a vital role in highly active research areas such as developing organometallic foldamers, designing molecules with potential biological applications, or mimicking structural biological motifs.[9,10] Oligoamides derived from α-amino acids and $Fn(COOH)_2$ (Fn = ferrocene-1,1′-diyl) (Scheme 2, type **III**)[11–24] or H_2N-Fn-COOH (Fca, 1′-amino-

Scheme 1. Turn Inducers (T) Constrain Parallel Ureidopeptide Strands, Which Are Held Together by IHBs (arrows point from N to C termini of peptide chains)

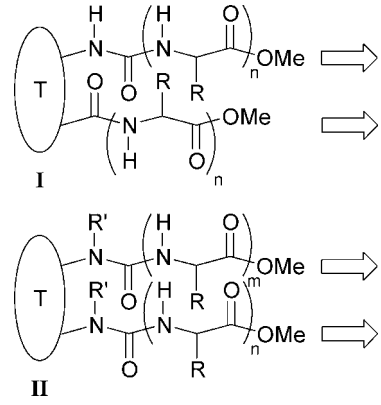

* Corresponding authors. (K.H.) Fax: int + 49 6221 545707. Tel. int + 49 6221 548587. E-mail: katja.heinze@urz.uni-heidelberg.de. (V.R.) Fax: int + 385 4836 082. E-mail: vrapic@pbf.hr.
† Department of Chemistry and Biochemistry, University of Zagreb.
‡ Department of Applied Chemistry, University of Zagreb.
§ University of Heidelberg.

(1) Liskamp, R. M. J. *Angew. Chem., Int. Ed. Engl.* **1994**, *33*, 305–307.
(2) Boeijen, A.; Liskamp, R. M. J. *Eur. J. Org. Chem.* **1999**, 2127–2135.
(3) Boeijen, A.; van Ameijele, J.; Liskamp, R. M. J. *J. Org. Chem.* **2001**, *66*, 8454–8462.
(4) Kruijtzer, J. A. W.; Lefeber, D. J.; Liskamp, R. M. J. *Tetrahedron Lett.* **1997**, *38*, 5335–5338.
(5) Burgess, K.; Ibarzo, J.; Linthicum, D. S.; Russell, D. H.; Shin, H.; Shitangkoon, A.; Totani, R.; Zhang, A. J. *J. Am. Chem. Soc.* **1997**, *119*, 1556–1564.
(6) North, M. *J. Peptide Sci.* **2000**, *6*, 301–313.
(7) Nowick, J. S. *Acc. Chem. Res.* **1999**, *32*, 287–296.
(8) Nowick, J. S.; Smith, E. M.; Noronha, G. *J. Org. Chem.* **1995**, *60*, 7386–7387.
(9) Moriuchi, T.; Hirao, T. *Chem. Soc. Rev.* **2004**, *33*, 294–301.
(10) van Staveren, D. R.; Metzler-Nolte, N. *Chem. Rev.* **2004**, *104*, 5931–5986.
(11) Lapić, J.; Siebler, D.; Heinze, K.; Rapić, V. *Eur. J. Inorg. Chem.* **2007**, 2014–2024.
(12) Chowdhury, S.; Sanders, D. A. R.; Schatte, G.; Kraatz, H.-B. *Angew. Chem., Int. Ed.* **2006**, *45*, 751–754.
(13) Moriuchi, T.; Nagai, T.; Hirao, T. *Org. Lett.* **2005**, *7*, 5265–5268.
(14) Kirin, S. I.; Wissenbach, D.; Metzler-Nolte, N. *New J. Chem.* **2005**, *29*, 1168–1173.
(15) Chowdhury, S.; Schatte, G.; Kraatz, H.-B. *Dalton Trans.* **2004**, 1726–1730.
(16) Appoh, F. E.; Sutherland, T. C.; Kraatz, H.-B. *J. Organomet. Chem.* **2004**, *689*, 4669–4677.
(17) Moriuchi, T.; Yoshida, K.; Hirao, T. *Org. Lett.* **2003**, *5*, 4285–4288.
(18) van Staveren, D. R.; Weyhermüller, T.; Metzler-Nolte, N. *Dalton Trans.* **2003**, 210–220.
(19) Moriuchi, T.; Nomoto, A.; Yoshida, K.; Hirao, T. *Organometallics* **2001**, *20*, 1008–1013.

10.1021/om700950r CCC: $40.75
Publication on Web 01/26/2008

Scheme 2. Parallel and Antiparallel Peptide Strands Tethered to Ferrocene as Turn Inducer via Amide and Ureylene Groups (X = OMe, AA-OMe; Y = Boc, Boc-AA; arrows point from N to C termini of the peptide chains)

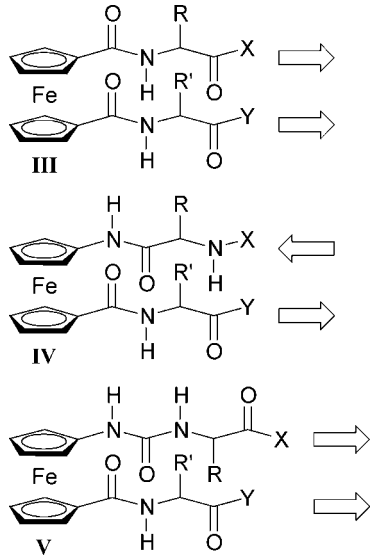

ferrocene-1-carboxylic acid) (Scheme 2, type **IV**)[25–33] can fold to β-strand analogous conformations with antiparallel or parallel peptide chains. Conjugates of Fca and α-amino acids were shown to bind anions via hydrogen bonding.[26,31] Self-assembly of amide-substituted ferrocenes into dimers, chains, and sheets has been observed in the solid state as well as in solution.[25,32] Generally, the interplay between intramolecular hydrogen bonding (folding) and intermolecular hydrogen bonding (self-assembly, guest binding) depends on the environment (solid state, solution, solvent, temperature, etc.). For ferrocene derivatives it is furthermore largely determined by the special rigidity/flexibility of the metallocene scaffold.

By replacing an amido group with a ureylene unit in type **IV** compounds ureidopeptides **V** are derived. In these analogues of type **I** compounds parallel strands are expected. Like the amide group, the ureylene moiety is highly suitable for the formation of hydrogen bonds, as it can act both as hydrogen donor and hydrogen acceptor. This property has been exploited

Scheme 3. Ferrocene-Containing Urea Derivatives

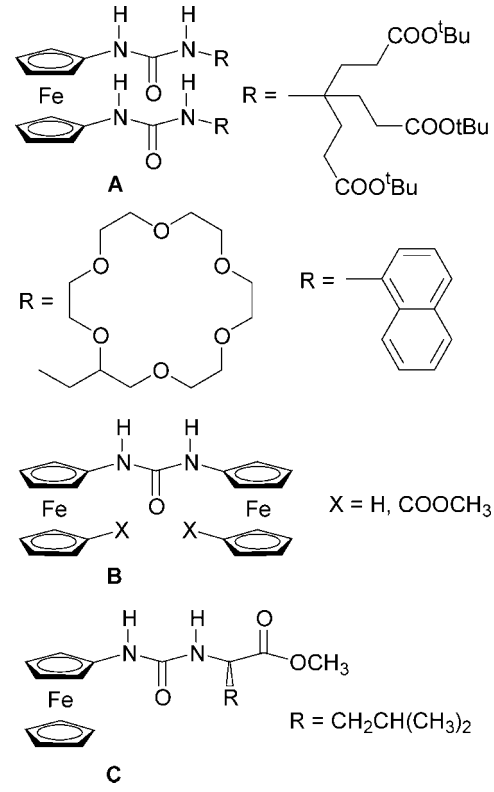

in anion binding chemistry and self-assembly processes.[34,35] Anion binding and anion sensing with ferrocene urea receptors (usually ferrocenylureas or symmetrically disubstituted (ferrocene-1,1′-diyl)bisureas, Scheme 3, **A**) has been pioneered by Tucker,[36] Beer,[37,38] Kaifer,[39] and Tárraga and Molina[40–43] with ferrocene as an electrochemical detection unit. Self-assembly of urea derivatives based on the complementary hydrogen donor NH and hydrogen acceptor CO groups has been utilized for example in the construction of ion channels.[44] The ureylene group has been studied by Kraatz as a linker between two ferrocene moieties (Scheme 3, **B**[45]) with respect to electron transfer and charge delocalization.[46] A chiral conjugate of ferrocene and Leu (Scheme 3, **C**) has been suggested by Schögl as model chromophor for the labeling of chiral amino com-

(20) Moriuchi, T.; Nomoto, A.; Yoshida, K.; Ogawa, A.; Hirao, T. *J. Am. Chem. Soc.* **2001**, *123*, 68–75.
(21) Moriuchi, T.; Nomoto, A.; Yoshida, K.; Hirao, T. *J. Organomet. Chem.* **1999**, *589*, 50–58.
(22) Nomoto, A.; Moriuchi, T.; Yamazaki, S.; Ogawa, A.; Hirao, T. *Chem. Commun.* **1998**, 1963–1964.
(23) Herrick, R. S.; Jarret, R. M.; Curran, T. P.; Dragoli, D. R.; Flaherty, M. B.; Lindyberg, S. E.; Slate, R. A.; Thornton, L. C. *Tetrahedron Lett.* **1996**, *37*, 5289–5292.
(24) Oberhoff, M.; Duda, L.; Karl, J.; Mohr, R.; Erker, G.; Fröhlich, R.; Grehl, M. *Organometallics* **1996**, *15*, 4005–4011.
(25) Heinze, K.; Siebler, D. *Z. Anorg. Allg. Chem.* **2007**, *633*, 2223–2233.
(26) Heinze, K.; Wild, U.; Beckmann, M. *Eur. J. Inorg. Chem.* **2007**, 617–623.
(27) Barišić, L.; Rapić, V.; Metzler-Nolte, N. *Eur. J. Inorg. Chem.* **2006**, 4019–4021.
(28) Barišić, L.; àkić, M.; Mahmoud, K, A.; Liu, Y.; Kraatz, H,.B.; Pritzkow, H.; Kirin, S. I.; Metzler-Nolte, N.; Rapić, V. *Chem.−Eur. J.* **2006**, *12*, 4965–4980.
(29) Chowdhury, S.; Schatte, G.; Kraatz, H.-B. *Angew. Chem., Int. Ed.* **2006**, *45*, 6882–6884.
(30) Heinze, K.; Beckmann, M. *Eur. J. Inorg. Chem.* **2005**, 3450–3457.
(31) Heinze, K.; Schlenker, M. *Eur. J. Inorg. Chem.* **2005**, 66–71.
(32) Heinze, K.; Schlenker, M. *Eur. J. Inorg. Chem.* **2004**, 2974–2988.
(33) Barišsić, L.; Dropučić, M.; Rapić, V.; Pritzkow, H.; Kirin, S. I.; Metzler-Nolte, N. *Chem. Commun* **2004**, 2004–2005.
(34) Gale, P. A. *Amide- and Urea-Based Anion Receptors, in Encyclopedia of Supramolecular Chemistry*; Taylor & Francis, 2004; p 31–41
(35) Kang, S. O.; Begum, R. A.; Bowman-James, K. *Angew. Chem., Int. Ed.* **2006**, *45*, 7882–7894.
(36) Miyaji, H.; Collonson, S. R.; Prokeš, I.; Tucker, J. H. R., *Chem. Commun.* **2003**, 64–65.
(37) Evans, A. J.; Matthews, S. E.; Cowley, A. R.; Beer, P. D. *Dalton Trans.* **2003**, 4644–4650.
(38) Pratt, M. D.; Beer, P. D. *Polyhedron* **2003**, *22*, 649–653.
(39) Moon, K.; Kaifer, A. E. *J. Am. Chem. Soc.* **2004**, *126*, 15016–15017.
(40) Otón, F.; Tárraga, A.; Espinosa, A.; Velasco, M. D.; Molina, P. *Dalton Trans.* **2006**, 3685–3692.
(41) Otón, F.; Tárraga, A.; Espinosa, A.; Velasco, M. D.; Molina, P. *J. Org. Chem.* **2006**, *71*, 4590–4598.
(42) Otón, F.; Tárraga, A.; Velasco, M. D.; Molina, P. *Dalton Trans.* **2005**, 1159–1161.
(43) Otón, F.; Tárraga, A.; Espinosa, A.; Velasco, M. D.; Bautista, D.; Molina, P. *J. Org. Chem.* **2005**, *70*, 6603–6608.
(44) Cazacu, A.; Tong, C.; van der Lee, A.; Fyles, T. M.; Barboiu, M. *J. Am. Chem. Soc.* **2006**, *128*, 9541–9548.
(45) Barišc, L.; Rapić, V.; Kovač, V. *Croat. Chem. Acta* **2002**, *75*, 199–210.
(46) Mahmoud, K.; Long, Y.-T.; Schatte, G.; Kraatz, H.-B. *J. Organomet. Chem.* **2004**, *689*, 2250–2255.

Scheme 4[a]

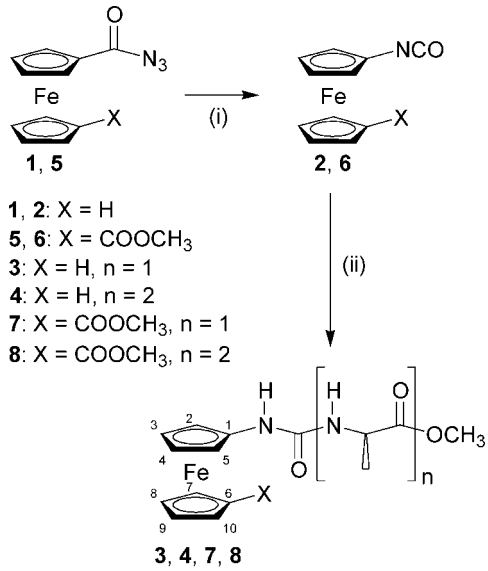

[a] (i) benzene, 80°C. (ii) $n = 1$: H-Ala-OCH_3·HCl, NEt_3, CH_2Cl_2; $n = 2$: H-Ala-Ala-OCH_3·HCl, NEt_3, CH_2Cl_2.

pounds such as peptides and proteins for the investigation of configurations with chiroptical methods.[47]

In this study we report the synthesis and conformational analysis of ferrocene ureidopeptides containing alanine or alanylalanine subunits, as well as of their 1′-methoxycarbonyl derivatives, as an entry into enantiomerically pure ferrocene-labeled anion receptors and β-strand models (organometallic peptidomimetics[10]) (Scheme 1, type **II**, T = Fn, and Scheme 2, type **V**). Folding versus self-assembly of the new ferrocene ureidopeptides is investigated with the aid of spectroscopic analysis (CD, IR, NMR spectroscopy), theoretical calculations, and X-ray structure analysis.

Results and Discussion

Synthesis of Ferrocene Ureidopeptides 3, 4, 7, and 8. The synthesis of ferrocene ureidopeptides **3**, **4**, **7**, and **8** is depicted in Scheme 4. The starting ferrocenecarboxazide **1** was prepared in 75% yield from ferrocenecarboxylic acid Fc−COOH by the successive action of $ClCOOEt/NEt_3$ in acetone and an aqueous solution of NaN_3 via the intermediate mixed anhydride.[48] Methyl 1′-azidocarboxylferrocene-1-carboxylate **5** was prepared in a similar fashion from 1′-methoxycarbonylferrocene-1-carboxylic acid, CH_3OOC−Fn−COOH, in 73% yield. Curtius rearrangement of **1** or **5** in benzene gave the corresponding isocyanates **2** and **6**, respectively.[48] The course of the reactions was easily monitored by IR spectroscopy, as characteristic absorption bands of **1/5** around (2138 and 1687 cm^{-1}) decrease while the band for the NCO substituent of **2/6** increases (2173 cm^{-1}). As prolonged heating results in formation of *N*,*N*′-diferrocenylureas of type **B** (Scheme 3),[45,46,49] the reactions could not be driven to completion. The formation of byproduct of type **B** can be explained by thermolysis of isocyanates **2/6** to the corresponding iron-stabilized nitrenes,[41] which then abstract hydrogen atoms from the reaction medium to give the corresponding amines.

Scheme 5. Possible Mechanism of the Formation of Symmetrical Ureas B from Isocyanates 2 and 6

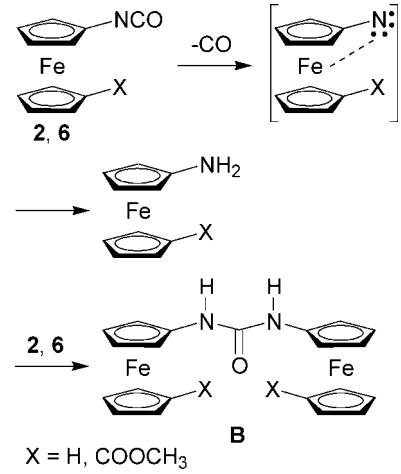

Nucleophilic addition of these amines to **2/6** results in the formation of symmetrical ureas of type **B** (Scheme 5).

Purification of **2** and **6** by chromatography proved to be difficult, as **1/2** and **5/6** possess almost identical R_f values. Thus crude product mixtures were employed in the coupling step with alanine and alanylalanine methyl esters to give **3**, **4**, **7**, and **8**, respectively. These products could be purified by thin-layer chromatography. The ureidopeptides **3**, **4**, **7**, and **8** were fully characterized by multinuclear and two-dimensional NMR spectroscopy, IR, UV/vis, and CD spectroscopy, as well as by high-resolution mass spectrometry (Tables 1, 2, 3, and 4).

Spectroscopic Analysis of Ferrocene Ureidopeptides 3, 4, 7, and 8. For all ureidopeptides **3**, **4**, **7**, and **8** the characteristic ferrocene absorption band is observed at 448 nm in CH_2Cl_2 (Table 1). Its energy is independent of the solvents employed [CH_2Cl_2, CH_3CN, CH_2Cl_2/DMSO (20% v/v)]. Around this absorption maximum the chiral compounds show either positive (**4**) or negative Cotton effects (**7**, **8**) in CH_2Cl_2, which corroborates the chiral environment around the ferrocene chromophores (Figure 1). For the leucine analogue of **3** (Scheme 3, **C**) Schlögl has also reported a positive Cotton effect at 459 nm in ethanol.[47]

Generally, the CD maxima are found at lower energy than the UV/vis maxima, which has been ascribed to the electronic splitting of the ferrocene absorption band.[47] In the presence of DMSO the CD maxima shift to even lower energy by 280 cm^{-1} (**4**), 220 cm^{-1} (**7**), and 210 cm^{-1} (**8**), although the UV/vis absorption maxima remain unchanged.

If a preferred folded conformation with intramolecular hydrogen bonds existed in CH_2Cl_2 solution, one should expect a decrease of the CD intensity in coordinating solvents which can compete for hydrogen-bonding sites and thus disrupt IHBs. This has been shown for several examples of chiral ferrocene peptides.[30] However, upon addition of DMSO, which is a strong competitor for NH hydrogen-bonding sites, to CH_2Cl_2 solutions of **4**, **7**, or **8**, the CD signals *increase* by a factor of 2 (**4**) and 1.6 (**7**) and the signal even switches the sign for compound **8** (Figure 1, Table 1). The latter observation suggests that the chromophore environment of **8** is substantially different in CH_2Cl_2 and CH_2Cl_2/DMSO. These observations clearly point to other ordering phenomena being responsible for the solvent-dependent Cotton effects observed than stable conformations with intramolecular hydrogen bonds in noncoordinating solvents. In the solid state (KBr disk) **4** (X = H) displays a positive Cotton effect at 460 nm, while **8** (X = $COOCH_3$) exhibits a negative

(47) Falk, H.; Krasa, C.; Schlögl, K. *Monatsh. Chem.* **1969**, *100*, 1552–1563.
(48) Schlögl, K.; Seiler, H. *Naturwiss.* **1958**, *45*, 337.
(49) Nesmeyanov, N. A.; Reutov, O. A. *Dokl. Akad. Nauk SSSR* **1957**, *115*, 518–521.

Table 1. UV/Vis and CD Data ($c = 10^{-3}$ M) of 4, 7, and 8 in CH_2Cl_2 and CH_2Cl_2/DMSO (20% v/v)

	solvent	4	7	8
λ_{max}/nm (ϵ/M^{-1} cm^{-1})	CH_2Cl_2	448 (370)	448 (340)	448 (230)
$\lambda\delta_{max}$/nm (ϵ/M^{-1} cm^{-1})	CH_2Cl_2/DMSO	448 (360)	448 (340)	448 (230)
λ_{max}/nm (M_θ/deg M^{-1} cm^{-1})	CH_2Cl_2	460 (+850)	478 (−2070)	483 (−1740)
λ_{max}/nm (M_θ/deg M^{-1} cm^{-1})	CH_2Cl_2/DMSO	466 (+1700)	483 (−3370)	488 (+1200)

Table 2. IR (in CH_2Cl_2; $c = 10^{-3}$ M) and HR-FAB Mass Spectrometric Data of 3, 4, 7, and 8

	3	4	7	8
ν_{NH} (free)/cm^{-1}	3426	3426	3419	3424
ν_{NH} (assoc.)/cm^{-1}	3367	3363	3370	3360
ν_{CO} (ester)/cm^{-1}	1740	1742	1740, 1706	1741, 1708
ν_{CO} (amide I)/cm^{-1}	1675	1682, 1677	1679	1683, 1677
molecular formula	$C_{15}H_{18}N_2O_3Fe$	$C_{18}H_{23}N_3O_4Fe$	$C_{17}H_{20}N_2O_5Fe$	$C_{20}H_{25}N_3O_6Fe$
m/*z* (obs)	330.0667	401.1038	388.0722	459.1093
m/*z* (calcd)	330.0667	401.1062	388.0732	459.1062

Table 3. ^{1}H NMR Chemical Shifts of 3, 4, 7, and 8 in CD_2Cl_2 ($c = 10^{-2}$ M, 400 MHz, atom numbering according to Scheme 4)[a]

	3	4	7	8
1-NH	5.63 (1H, s)	6.48 (1H, s)	6.40 (1H, s)	6.72 (1H, s)
NH_{Ala1}	5.70 (1H, d, 6.6 Hz)	6.09 (1H, d, 7.7 Hz)	5.60 (1H, d, 7.6 Hz)	5.79 (1H, d, 7.6 Hz)
NH_{Ala2}		7.07 (1H, d, 7.1 Hz)		7.12 (1H, d, 7.2 Hz)
$CH_{\alpha, Ala1}$	4.46 (1H, dq, 6.6, 7.2 Hz)	4.47 (1H, dq, 7.1, 7.2 Hz)	4.49 (1H, dq, 7.6, 7.2 Hz)	4.48 (1H, dq, 7.2, 7.2 Hz)
$CH_{\alpha, Ala2}$		4.49 (1H, dq, 7.7, 7.2 Hz)		4.50 (1H, dq, 7.6, 7.0 Hz)
H^2, H^5	4.37 (2H, bs)	4.38 (1H, bs), 4.35 (1H, bs)	4.47 (1H, pt), 4.42 (1H, pt)	4.52 (1H, ddd, 2.6, 1.2, 1.2 Hz), 4.40 (1H, ddd, 2.6, 1.2, 1.2 Hz)
H^3, H^4	4.14 (2H, bs)	4.05 (2H, bs)	4.06 (2H, pt)	4.04 (1H, ddd, 3.9, 2.6, 1.2 Hz), 4.02 (1H, ddd, 3.9, 2.6, 1.2 Hz)
H^7, H^{10}	4.27 (5H, s)	4.21 (5H, s)	4.82 (2H, pt)	4.81 (2H, pt)
H^8, H^9			4.45 (2H, pt)	4.43 (2H, pt)
1-OCH_3	3.73 (3H, s)	3.72 (3H, s)	3.74 (3H, s)	3.72 (3H, s)
1′-OCH_3			3.78 (3H, s)	3.77 (3H, s)
$CH_{3, Ala1}$	1.40 (3H, d, 7.2 Hz)	1.40 (3H, d, 7.0 Hz)	1.41 (3H, d, 7.2 Hz)	1.41 (3H, d, 7.0 Hz)
$CH_{3, Ala2}$		1.39 (3H, d, 7.2 Hz)		1.40 (3H, d, 7.2 Hz)

[a] Chemical shifts and coupling constants of superimposed proton signals H^2/H^5 and CHα were obtained via spectral simulation of the multiplets. All assignments are based on COSY, TOCSY, and NOESY spectra.

Table 4. ^{13}C NMR Chemical Shifts of 3, 4, 7, and 8 in CD_2Cl_2 ($c = 10^{-2}$ M, 100 MHz, atom numbering according to Scheme 4)[a]

	3[a]	4	7	8
FcCO			171.59 (s)	171.62 (s)
CO_{ester}	174.51 (s)	173.13 (s)	173.84 (s)	173.18 (s)
COurea	156.00 (s)	156.22 (s)	155.35 (s)	155.67 (s)
CO_{amide}		173.10 (s)		173.07 (s)
$C_{\alpha, Ala1}$	48.81 (s)	49.58 (s)	48.97 (s)	49.55 (s)
$C_{\alpha, Ala2}$		48.26 (s)		48.31 (s)
C^1	n.o.	n.o.	96.47 (s)	97.07 (s)
C^2, C^5	63.17 (s), 62.74 (s)	62.74 (s), 62.54 (s)	63.77 (s), 63.62 (s)	63.33 (s), 62.96 (s)
C^3, C^4	65.92 (s), 65.83 (s)	65.22 (s)	66.70 (s), 66.65 (s)	66.51 (s), 66.35 (s)
C^6	70.32 (s)	n.o.	72.48 (s)	72.38 (s)
C^7, C^{10}	69.77 (s)	69.37 (s)	71.12 (s)	71.07 (s)
C^8, C^9			72.12 (s)	72.44 (s)
1-OCH_3	52.41 (s)	52.35 (s)	52.32 (s)	52.35 (s)
1′-OCH_3			51.69 (s)	51.68 (s)
$CH_{3, Ala1}$	18.99 (s)	18.72 (s)	18.59 (s)	18.85 (s)
$CH_{3, Ala2}$		17.85 (s)		17.75 (s)

[a] In $CDCl_3$.

Cotton effect at 483 nm, analogous to the effects observed in CH_2Cl_2 solution (Figure 1 and Supporting Information).

To shed some light onto the possible folding or self-assembly of ureidopeptides in solution, IR and detailed NMR spectroscopic analyses were undertaken (Tables 2, 3, 4, and 5). In CH_2Cl_2 solution ($c = 10^{-3}$ M) signals for NH stretching vibrations are observed around 3420 (m) and 3350 cm^{-1} (w), indicative of free and hydrogen-bonded NH groups, respectively (Table 2). In the solid state absorptions of NH stretching vibrations are found below 3400 cm^{-1}, showing that all NH groups are involved in hydrogen-bonding interactions. The carbonyl absorption of the amino acid esters are found at 1740 cm^{-1} in solution and below 1740 cm^{-1} in the solid state, suggesting that in the solid state hydrogen bonds to these ester groups are present. The CO stretching vibration of the 1′-ferrocene ester group occurs around 1710 cm^{-1} both in solution and in the solid, which indicates absence of hydrogen bonds to that CO functional group. Thus hydrogen bonds (either intra- or intermolecular) from NH groups to carbonyl substituents could be formed with the amino acid part of the molecules.

^{1}H and ^{13}C NMR spectra of the ureidopeptides display all signals expected for the proposed composition (Tables 3 and 4). Superimposed multiplets in the proton spectra have been deconvoluted by spectral simulation techniques, and assignments are based on two-dimensional NMR spectra. The chiral alanine unit renders the protons H^2/H^5 and H^3/H^4 as well as the

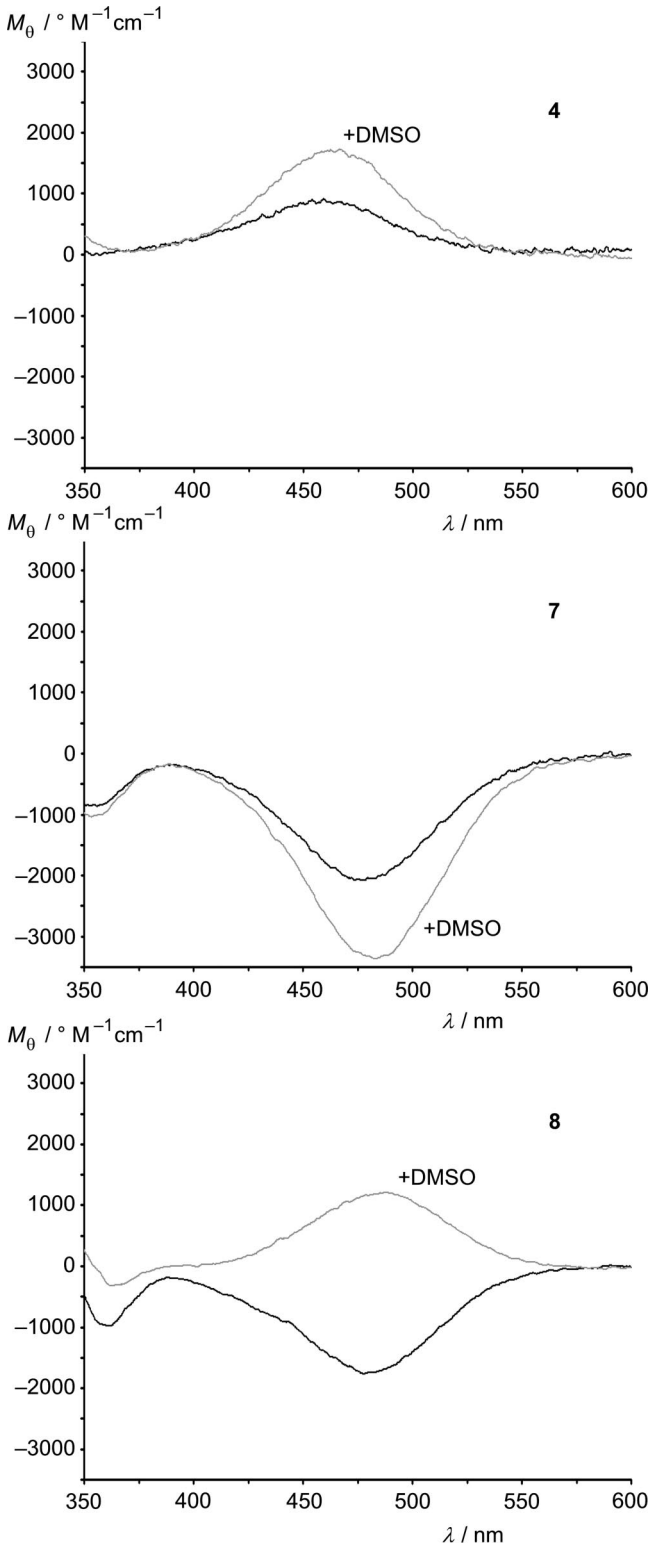

Figure 1. CD spectra of **4**, **7**, and **8** in CH_2Cl_2 and CH_2Cl_2/DMSO (20% v/v).

corresponding carbon atoms C^2/C^5 and C^3/C^4 of the N-substituted Cp ring diasterotopic, which is clearly visible in the spectra of **7** and **8** and partially resolved in the spectra of **3** and **4**. However, the signals of the proton pairs H^7/H^{10} and H^8/H^9 in the 1,1′-disubstituted ferrocenes **7** and **8** are indistinguishable (Table 3). The same holds for the corresponding resonances of the carbon atoms C^7/C^{10} and C^8/C^9 (Table 4). This contrasts with findings for α-amino acid conjugates of the type CH_3OOC-CHR-NH-CO-Fn-$NHCOCH_3$ [R = $CH(CH_3)_2$, $CH(CH_3)$-(C_2H_5)].[30] In these cases the hydrogen and carbon atoms of the Cp ring with the chiral substitutent as well as the hydrogen and carbon atoms of the $NHCOCH_3$-substituted Cp ring are diasterotopic and give rise to distinctly dispersed signals in the ^1H NMR and ^{13}C NMR spectra. This has been ascribed to IHBs between the two substituents transferring chiral information to both cyclopentadienyl rings. Thus for **7** and **8** the number of signals observed does not support IHBs, which also fits to the absence of any NOE cross-peak between the ferrocene ester CH_3 group and protons of the chiral substituent in the NOESY spectra of **7** and **8**. This interpretation is also in accordance with the IR data showing that the 1′-ferrocene ester group does not engage in hydrogen bonds at all.

Equilibration between hydrogen-bonded and non-hydrogen-bonded states in CD_2Cl_2 for a given NH proton is usually fast on the NMR time scale, and observed proton chemical shifts are weighted averages of the chemical shifts of contributing states. The proton chemical shifts of NH groups are found at δ 7.2 in dilute CD_2Cl_2 solution at 25 °C, suggesting only weak if any hydrogen bonding under these conditions. Upon cooling, all the NH signals are shifted to lower field with quite high temperature dependence (Figure 2, Table 5), indicative of intermolecular hydrogen bonds. Likewise in [D_6]-DMSO all NH signals are shifted to lower field due to the formation of $NH\cdots OSMe_2$ hydrogen bonds (Table 5).

Dilution experiments conducted on CD_2Cl_2 solutions of **4**, **7**, and **8** showed a downfield shift of NH protons upon increasing concentration, which is indicative of self-association through intermolecular hydrogen bonds (Figure 3). No plateaus have been observed in the concentration-dependent chemical shifts of NH protons such that distinct oligomers with definite stoichiometry are unlikely [which has been observed for benzo(ureido) crown-ethers].[44] We assume that the initial process is the formation of a dimer from two monomers. The data can be fit using this model with two chemical shifts, δ(monomer) and δ(dimer), and one formation constant, K_D, as unknowns. Association constants K_D and chemical shifts for numerical fits to the monomer/dimer model are compiled in Table 5. Interestingly, the association constants K_D derived from protons 1-NH and NH_{Ala1} (the ureylene group) are all very similar (**4**, **8**: 90 M^{-1}; **7**: 30 M^{-1}), while K_D derived from proton NH_{Ala2} (in **4** and **8**) is much lower. This indicates that both NH protons of the urea group interact almost synchronously, while the NH_{Ala2} proton interacts to a lesser extent. However, it appears that the second alanine moiety stabilizes the interaction of the urea group with hydrogen acceptors, which points to some cooperative hydrogen bonding involving all NH protons.

Thus, all the experimental data acquired suggest that **7** and **8** have no preferred conformation with IHBs in methylene chloride solution but self-assemble via intermolecular hydrogen bonds to dimers (and possibly finally to larger oligomers or polymers, *vide infra*) at higher concentrations. DMSO disrupts these intermolecular hydrogen bonds and disassembles the dimer (oligomer) to DMSO-solvated monomers. This interpretation also accounts for the unusual changes of CD signals when switching the solvent from CH_2Cl_2 to CH_2Cl_2/DMSO (*vide supra*) and is also in accord with the Cotton effects observed in solution and in the solid state.

DFT Calculations of 7 and 8. DFT calculations have been quite successful in describing the energetics of IHBs in 1,1′-disubstituted ferrocenes.[11,25,26,30–32,50] Thus several conforma-

(50) Heinze, K.; Beckmann, M. *J. Organomet. Chem.* **2006**, *691*, 5576–5584.

Table 5. Temperature-Dependent, Solvent-Dependent, and Concentration-Dependend ^{1}H NMR Data of NH Protons of 4, 7, and 8

compound	proton	$\Delta\delta$/ppb K^{-1}	δ/([D$_6$]-DMSO) δ (CD_2Cl_2)/ppm	K_D/M^{-1}	δ(monomer)/ppm	δ(dimer)/ppm	R^2
4	1-NH	−15.4	1.25	115 ± 9	5.55 ± 0.02	6.51 ± 0.02	0.9996
	NH_{Ala1}	−11.1	0.08	84 ± 7	5.58 ± 0.01	6.16 ± 0.02	0.9996
	NH_{Ala2}	−17.3	1.37	41 ± 3	6.61 ± 0.01	7.33 ± 0.02	0.9996
7	1-NH	−14.6	1.34	32 ± 5	5.70 ± 0.01	6.47 ± 0.06	0.9994
	NH_{Ala1}	−9.1	0.77	35 ± 6	5.23 ± 0.01	5.62 ± 0.03	0.9993
8	1-NH	−16.8	1.10	91 ± 13	5.76 ± 0.03	6.81 ± 0.05	0.9982
	NH_{Ala1}	−16.4	0.40	81 ± 11	5.19 ± 0.02	6.08 ± 0.04	0.9983
	NH_{Ala2}	−20.2	1.25	26 ± 3	6.69 ± 0.01	7.54 ± 0.05	0.9986

tions of **7** and **8** with and without IHBs were calculated at the B3LYP/Lanl2DZ level of theory (Figure 4). No energetically preferred conformation could be located, as all calculated geometries of **7** possess a similar energy within an energy band of 8 kJ mol^{-1}. This corroborates the interpretation based on experimental data (IR, NMR) that intermolecular hydrogen bonds are favored over IHBs.

For the alanylalanine derivative **8** additional IHBs involving NH_{Ala2} are in principle possible (Figure 5). However, the conformations **8-A**, **8-A′**, **8-B**, **8-B′**, and **8-C** are also not significantly preferred over conformation **8-C′** without IHBs. Thus in solution **7** and **8** are best described as a dynamic mixture of energetically similar conformers.

X-ray Crystal Structure of 8. **8** crystallized in the triclinic space group *P*1 with a Flack parameter of 0.075(16). The absolute configuration of the asymmetric carbon atoms C14 and C17 of the two alanyl moieties is *S* (Figure 6). Bond distances are within expected values for all structural moieties within the molecule (Cp rings, urea fragment, Ala and $COOCH_3$ units). As found in methylene chloride solution intramolecular hydrogen bonds are absent in the crystal. However, intermolecular hydrogen bonds are found between molecules translated along the *a* axis via N2−(H12N) and N3−(H13N) as hydrogen donor groups to carbonyl oxygen atoms O4 and O5 as hydrogen acceptors, giving rise to chains of molecules connected by 12-membered rings (Figure 7, Table 6). The N1−(H1N1)···O4 distance is larger than 2.7 Å probably due to the formation of this unstrained hydrogen-bonded ring. As the urea moiety is almost planar with both NH groups oriented in the same direction the N1−(H1N1) vector also points to O4. Thus in the solid state only the peptide fragment is involved in hydrogen bonding, while the ferrocene-substituted ester moiety does not participate, which nicely fits the observations made in methylene

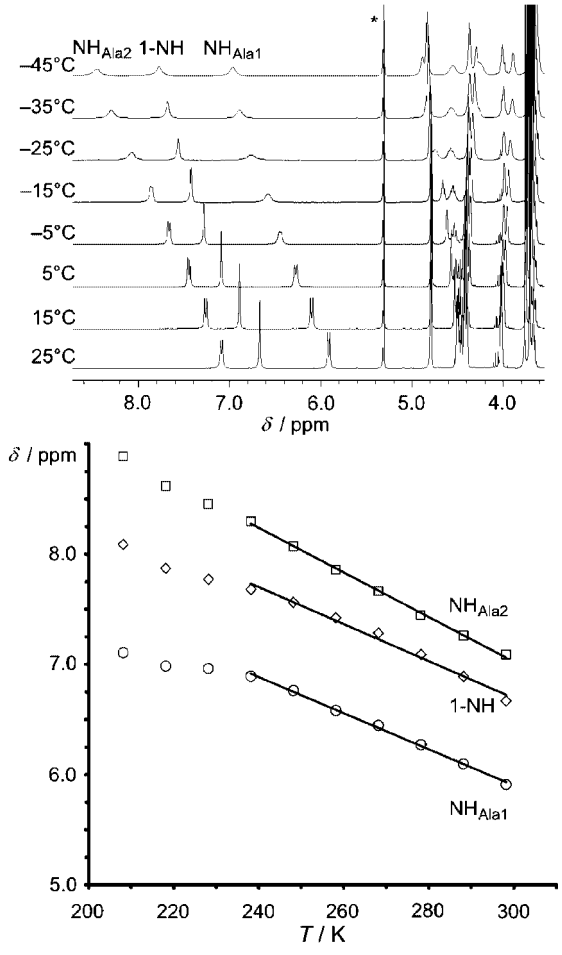

Figure 2. Partial VT ^{1}H NMR spectra of **8** in CD_2Cl_2 (top, * denotes residual $CHDCl_2$, 300 MHz) and δ versus *T* plot of amide proton signals.

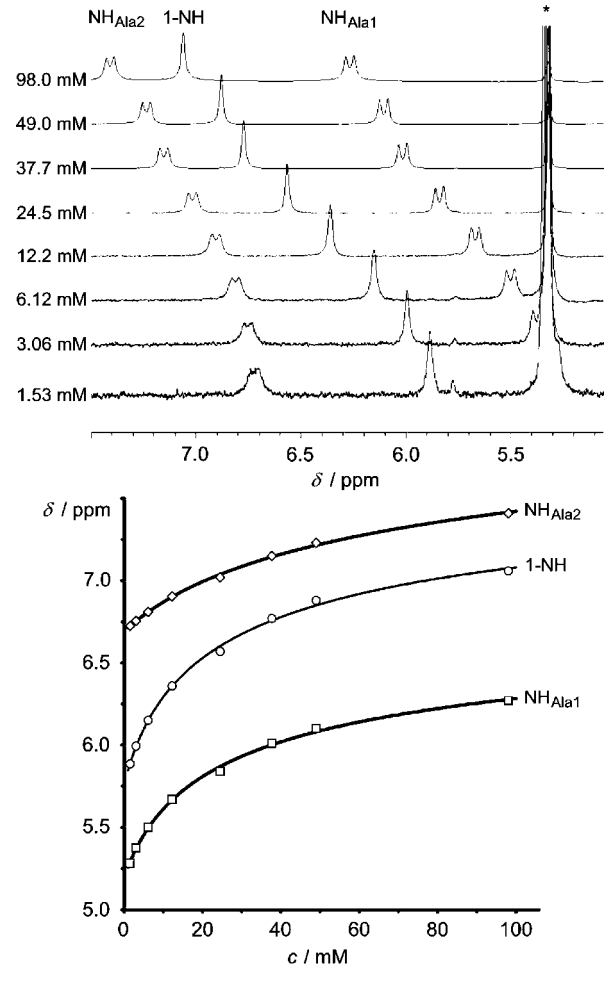

Figure 3. Partial concentration-dependent ^{1}H NMR spectra of **8** in CD_2Cl_2 (top, * denotes residual $CHDCl_2$, 200 MHz) and δ versus *c* plot of amide proton signals (the lines are fits to a dimerization model).

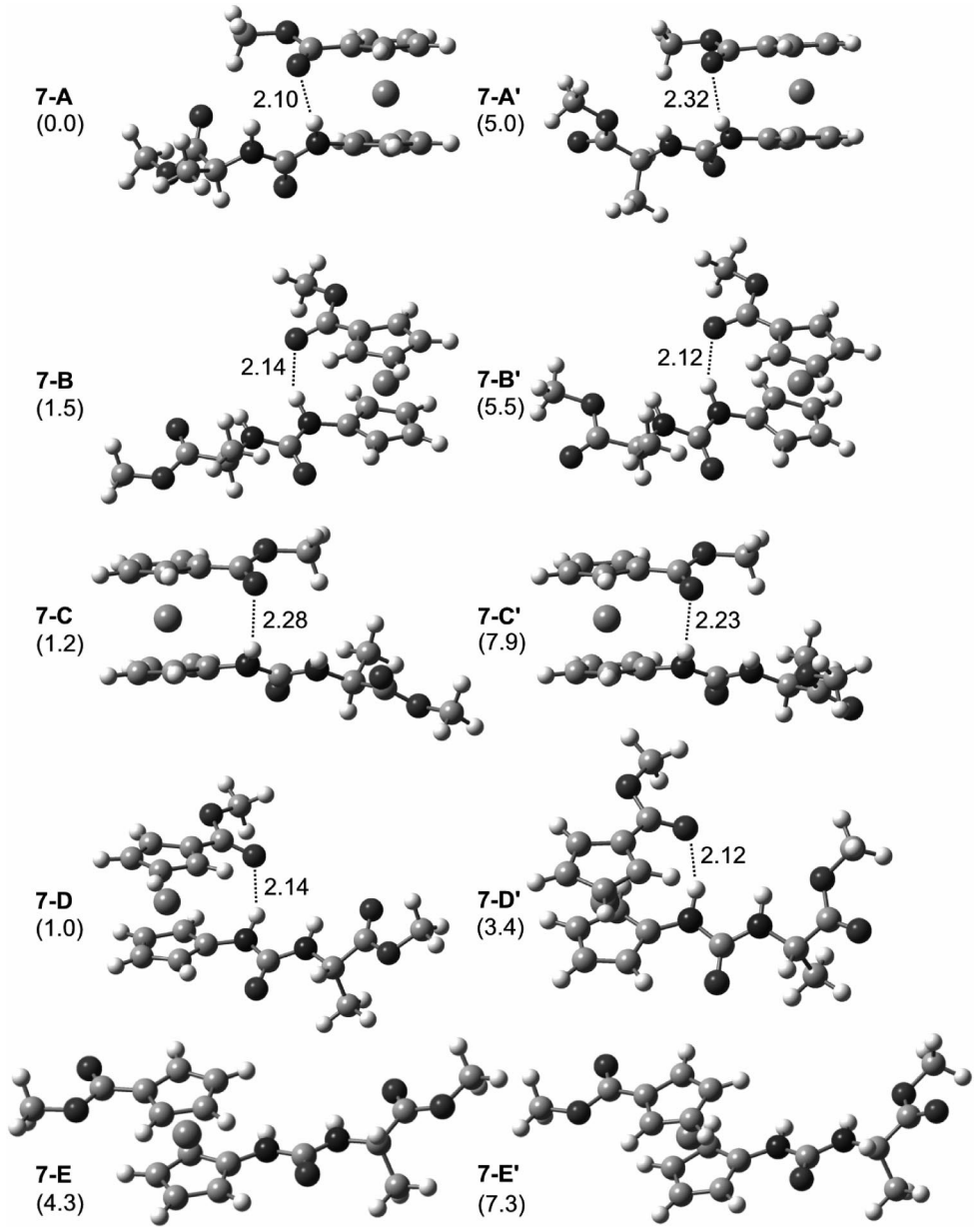

Figure 4. DFT-calculated minimum structures of **7** (relative energies in kJ mol^{-1} in parentheses; O···H distances in Å).

chloride solution. The bis(ferrocene) urea derivative CH_3OOC-Fn-NHCONH-Fn-$COOCH_3$ also engages in intermolecular hydrogen bonding in the crystal, however, involving interactions between the methyl ester substitutent of one Cp ring to the urea NH of an adjacent molecule, which results in the formation of a one-dimensional chain.[46] The hydrogen-bonded chain found for the crystal of **8** also supports the model employed for the concentration-dependent proton chemical shifts (*vide supra*).

Conclusion

Synthesis and conformational analysis of ferrocene ureidopeptides containing a 1′-methoxycarbonyl group as potential hydrogen acceptor in intra- or intermolecular hydrogen bonds have been performed. Thorough spectroscopic and theoretical studies of these systems revealed that (on the contrary to type **I** and **II** compounds, Scheme 1) intramolecular hydrogen bonds play only a minor role, while self-assembly processes prevail in solution and in the solid state. In these intermolecular hydrogen bonds urea NH groups are acting as hydrogen donors and alanine amide and ester CO groups play the role of hydrogen acceptors. The ester substituent in the 1′ position of the ferrocene is not involved in hydrogen bonding. Replacement of the 1′-ferrocene ester moiety by a peptide fragment giving C_2-symmetric ferrocene ureidopeptides (Scheme 1, type **II**, T = Fn; $n = m$) and type **V** conjugates (Scheme 2) to possibly induce IHBs with formation of stable conformations in solution is currently in progress in our laboratories.

Experimental Section

General Procedures. The syntheses were carried out under argon. CH_2Cl_2 used for synthesis and FT-IR spectroscopy was dried (P_2O_5), distilled over CaH_2, and stored over molecular sieves (4 Å). EDC, HOBt (Aldrich), and amino acid esters and amides (Merck) were used as received. Products were purified by preparative thin-layer chromatography on silica gel (Merck, Kieselgel 60 HF_{254}) using the mixtures CH_2Cl_2/EtOAc or CH_2Cl_2/MeOH. Melting points were determined with a Bucchi apparatus. IR spectra were recorded as CH_2Cl_2 solutions with a Bomem MB 100 mid FT-IR spectrophotometer. ^{1}H and ^{13}C{^{1}H} NMR spectra were

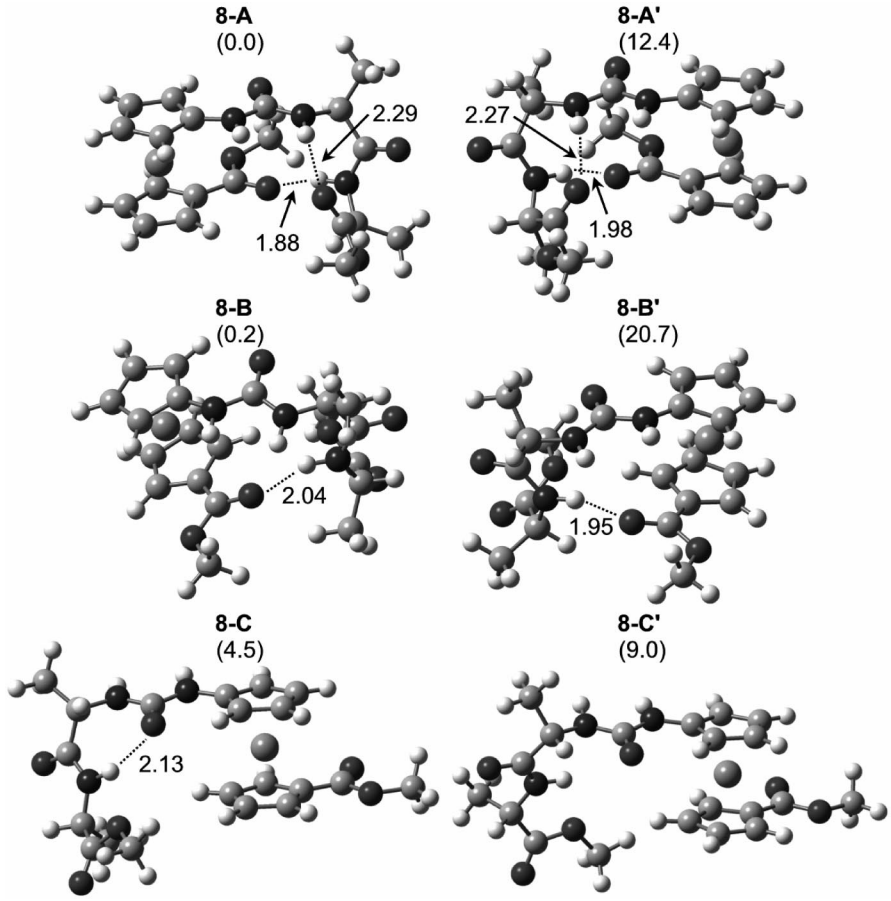

Figure 5. DFT-calculated minimum structures of **8** (relative energies in kJ mol^{-1} in parentheses; O···H distances in Å).

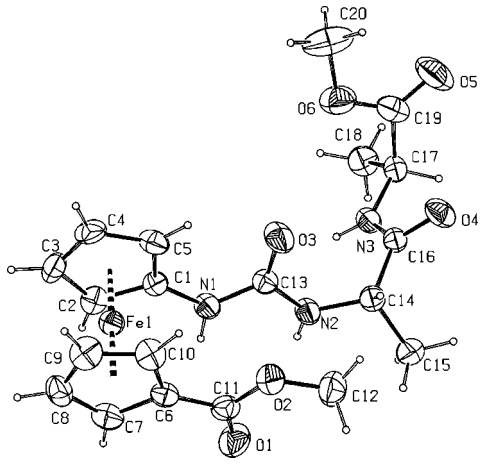

Figure 6. Molecular structure of **8** in the crystal.

recorded on a Varian EM 360 or Varian Gemini 300 spectrometer in CD_2Cl_2, $CDCl_3$, and [D_6]-DMSO solutions with Me_4Si as internal standard or on a Varian Unity Plus 400 spectrometer. FAB and HR-FAB mass spectra were recorded on a JEOL JMS-700. CD spectra were recorded with a Jasco-810 CD spectrophotometer.

Computational Method. Density functional calculations were carried out with the Gaussian03/DFT[51] series of programs. The B3LYP formulation of density functional theory was used employing the Lanl2DZ basis set.[51] All points were characterized as minima ($N_{imag} = 0$) by frequency analysis.

X-ray Crystal Structure Analysis. The data collection was carried out on an Xcalibur four-circle kappa geometry single-crystal diffractometer with an Xcalibur Sapphire 3 CCD detector by applying the CrysAlis Software system, Version 171.26, at ambient temperature.[52] Data reduction has been performed by the same program.[52] The data have been corrected for Lorentz polarization and scaled for absorption effects. The structure was solved by direct methods.[53] Refinement procedure by full-matrix least-squares methods based on F^2 values against all reflections has been performed including anisotropic displacement parameters for all non-H atoms.[54] The positions of hydrogen atoms belonging to the cyclopentadienyl Csp^2 and methyl and tetrahedral Csp^3 atoms were geometrically optimized applying the riding model [Csp^2-H, Csp^3(methyl)-H, Csp^3(tetrahedral)-H 0.93, 0.98, and 0.96 Å, respectively; $U_{iso}(H) = 1.2$ (for Csp^2 and Csp^3 (tetrahedral) and 1.5 for Csp^3(methyl) $U_{eq}(C)$]. The hydrogen atoms belonging to the nitrogen atoms N1, N2, and N3 have been found in the electron-density Fourier maps and refined freely [being in the range N-H =

(51) Frisch, M. J.; Trucks, G. W.; Schlegel, H. B.; Scuseria, G. E.; Robb, M. A.; Cheeseman, J. R.; Montgomery, J. A., Jr.; Vreven, T.; Kudin, K. N.; Burant, J. C.; Millam, J. M.; Iyengar, S. S.; Tomasi, J.; Barone, V.; Mennucci, B.; Cossi, M.; Scalmani, G.; Rega, N.; Petersson, G. A.; Nakatsuji, H.; Hada, M.; Ehara, M.; Toyota, K.; Fukuda, R.; Hasegawa, J.; Ishida, M.; Nakajima, T.; Honda, Y.; Kitao, O.; Nakai, H.; Klene, M.; Li, X.; Knox, J. E.; Hratchian, H. P.; Cross, J. B.; Adamo, C.; Jaramillo, J.; Gomperts, R.; Stratmann, R. E.; Yazyev, O.; Austin, A. J.; Cammi, C.; Pomelli, R.; Ochterski, J. W.; Ayala, P. Y.; Morokuma, K.; Voth, G. A.; Salvador, P.; Dannenberg, J. J.; Zakrzewski, V. G.; Dapprich, S.; Daniels, A. D.; Strain, M. C.; Farkas, O.; Malick, D. K.; Rabuck, A. D.; Raghavachari, K.; Foresman, J. B.; Ortiz, J. V.; Cui, Q.; Baboul, A. G.; Clifford, S.; Cioslowski, J.; Stefanov, B. B.; Liu, G.; Liashenko, A.; Piskorz, P.; Komaromi, I.; Martin, R. L.; Fox, D. J.; Keith, T.; Al-Laham, M. A.; Peng, C. Y.; Nanayakkara, A.; Challacombe, M.; Gill, P. M. W.; Johnson, B.; Chen, W.; Wong, M. W.; Gonzalez, C.; Pople, J. A. *Gaussian 03*, revision B.03; Gaussian, Inc.: Pittsburgh, PA, 2003.

(52) CrysAlis Software System, Version 171.23; Oxford Diffraction Ltd., 2004.

(53) Sheldrick, G. M. *Acta Crystallogr.* **1990**, *46*, 467–473.

(54) Sheldrick, G. M.; *SHELXL97* Program for the Refinement of Crystal Structures; University of Göttingen: Germany, 1997.

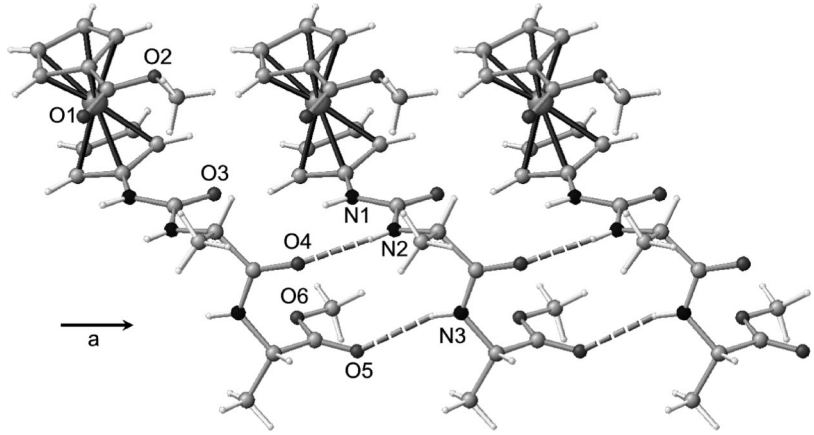

Figure 7. Intermolecular hydrogen bonds in the crystal of **8**.

Table 6. Intermolecular Hydrogen Bonds in the Crystal of 8

D−H···A	D−H/Å	H···A/Å	D···A/Å	D−H···A/deg	symmetry code
N2−H12N···O4	0.74(4)	2.11(4)	2.844(4)	175(4)	1+*x*, *y*, *z*
*N*3−H13N···O5	0.83(8)	2.34(8)	3.138(5)	162(7)	1+*x*, *y*, *z*

Table 7. Crystal Data for 8

formula	$C_{20}H_{25}FeN_3O_6$
M_r	459.28
color and habit	orange prism
cryst syst, space group	triclinic, *P*1
temp (K)	295
a (Å)	5.9735(13)
b (Å)	8.0852(17)
c (Å)	10.8924(19)
α (deg)	101.770(16)
β (deg)	90.204(17)
γ (deg)	95.378(18)
V (Å^3)	512.60(18)
Z	1
density (g cm^{-3})	1.488
μ (mm^{-1})	0.8
F(000)	240
θ range for data collection (deg)	4.5 to 30.0
h,*k*,*l* range	−8 to 7 ; −11 to 11 ; −15 to 14
no. measd reflns	7490
no. indep reflns (R_{int})	4977, 0.043
no. obsd reflns, $I \geq 2\sigma(I)$	4611
R, *wR* [$I \geq 2\sigma(I)$]	0.0473, 0.1236
R, *wR* [all data]	0.0509, 0.1278
goodness of fit on F^2, *S*	1.05
max., min. electron density (e Å^{-3})	−0.54, 0.60
Flack param	0.075(16)

0.74(4) to 0.85(5) Å]. CCDC-659841 contains the supplementary crystallographic data of **8**. These data can be obtained free of charge from the Cambridge Crystallographic Data Centre via www.ccdc.cam.ac.uk/data_request.cif.

Ferrocenecarboxazide Fc-CO-N$_3$ (1). Ferrocenecarboxylic acid (400 mg, 1.74 mmol) was suspended in water (0.3 mL), and sufficient acetone was added to dissolve it. After cooling to 0 °C, triethylamine (202 mg, 2.0 mmol) in acetone (3.3 mL) was added. While maintaining the temperature at 0 °C, a solution of ethyl chloroformate (242 mg, 2.23 mmol) in the same solvent (0.9 mL) was added. After stirring for 30 min at 0 °C a solution of sodium azide (173 mg, 2.63 mmol) in water was added. After stirring for 1 h at 0 °C the mixture was poured into ice–water and extracted with methylene chloride. The extracts were washed with 5% aqueous solution of $NaHCO_3$ and a saturated aqueous solution of NaCl, dried over $NaSO_4$, and evaporated *in vacuo* at room temperature to dryness to leave red crystals (332 mg, 75%). Mp: 84–86 °C. IR (CH_2Cl_2): *ν* 2138 (s, N_3), 1687 (s, CO_{azide}) cm^{-1}. ^{1}H NMR ($CDCl_3$): *δ* 4.83 (s, 2H, H^{2,5}), 4.52 (s, 2H, H^{3,4}), 4.27 (s, 5H, Cp−H).

Isocyanatoferrocene Fc-NCO (2). A solution of ferrocenecarboxazide **1** (400 mg, 1.56 mmol) in dry benzene (20 mL) was heated to 85 °C for 4 h. After cooling to 20 °C, the reaction mixture was evaporated *in vacuo* to dryness. This crude product was applied for the following coupling reactions without further purification. IR (CH_2Cl_2): *ν* 2173 (s, NCO) cm^{-1}.

Fc-NH-CO-Ala-OCH$_3$ (3). To a suspension of crude **2** (140 mg) in dry methylene chloride was added H-Ala-OCH_3 [obtained from H-Ala-OCH_3·HCl (130 mg, 1 mmol) by treatment with Et_3N in CH_2Cl_2]. The mixture was stirred for 1 h at room temperature. The reaction mixture was washed with saturated aqueous $NaHCO_3$ and water. The organic layer was dried over Na_2SO_4 and evaporated *in vacuo*. TLC purification with CH_2Cl_2/EtOAc (10:1) gave 47 mg (36%) of orange crystals and 49 mg of compound **1**. Mp: 154–157 °C. FAB-MS: *m*/*z* (%) 330 (100, M$^+$), 315 (77), 298 (95).

Fc-NH-CO-Ala-Ala-OCH$_3$ (4). A solution of Boc-Ala-Ala-OCH_3 (380 mg, 1.5 mmol) in AcOEt was deprotected by treating with gaseous HCl. H-Ala-Ala-OCH_3·HCl resulting after evaporation of the solvent was treated with Et_3N in CH_2Cl_2 and coupled with crude isocyanatoferrocene **2** (300 mg). The mixture was stirred for 1 h at room temperature and washed with saturated aqueous $NaHCO_3$ and water. The organic layer was dried over Na_2SO_4 and evaporated *in vacuo*. TLC purification with CH_2Cl_2/EtOAc (10:1) gave 180 mg (42%), yellow crystals, followed by 130 mg of **1**. Mp: 142–145 °C. IR (KBr): *ν* 3356, 3296 (m, NH, assoc.), 1735 (s, CO_{ester}), 1636 (s, amide I), 1557 (s, amide II) cm^{-1}. FAB-MS: *m*/*z* (%) 401 (100, M$^+$). Anal. Calcd for $C_{18}H_{23}FeN_3O_4$: C, 53.88; H, 5.78; N, 10.50. Found: C, 54.00; H, 6.16; N, 10.56.

Methyl 1′-azidocarbonylferrocene-1-carboxylate (5). In a similar way to the preparation of ferrocenecarboxazide **1**, starting from 1′-methoxycarbonylferrocene-1-carboxylic acid (1.2 g, 4.2 mmol) **5** was obtained in the form of red crystals (947 mg, 73%). Mp: 101–102 °C. IR (CH_2Cl_2): *ν* 2138 (s, N_3), 1717 (s, CO_{ester}), 1687 (s, CO_{azide}) cm^{-1}. ^{1}H NMR ($CDCl_3$): *δ* 4.87 (2H, s, H$^{2',5'}$), 4.85 (2H, s, H^{2,5}), 4.54 (2H, s, H$^{3-4}$), 4.45 (2H, s, H$^{3',4'}$), 3.83 (3H, s, $COOCH_3$). ^{13}C NMR, APT ($CDCl_3$): *δ* 175.90 (s, CO_{azide}), 170.29 (s, CO_{ester}), 74.07 (s, C$^{1'}$), 73.66 (s, C^{2,5}), 73.04 (s, C^1), 72.72 (s, C$^{2',5'}$), 71.81 (s, C^{3,4}), 71.75 (s, C$^{3',4'}$), 51.96 (s, CH_3).

Methyl-1′-isocyanatoferrocene-1-carboxylate (6). Similarly to the preparation of isocyanatoferrocene **2** a benzene solution of **5** (180 mg, 0.632 mmol) gave 170 mg of crude compound **6** contaminated with **5**. IR (CH_2Cl_2): *ν* 2173 (s, NCO), 1717 (s, CO_{ester}) cm^{-1}.

CH_3OOC-Fn-NH-CO-Ala-OCH_3 (7). The crude compound **6** (170 mg) was suspended in dry methylene chloride and coupled with H-Ala-OCH_3 (obtained from H-Ala-OCH_3·HCl by treatment

with Et_3N in CH_2Cl_2). The mixture was stirred for 1 h. After standard workup, the product was purified by TLC [CH_2Cl_2/EtOAc (10:1)], yielding 90 mg (48%) of **7** (orange resin) followed by 40 mg of azide **5**. FAB-MS: *m*/*z* (%) 388 (100, M^+). Anal. Calcd for $C_{17}H_{20}FeN_2O_5$: C, 52.60; H, 5.19; N, 7.22. Found: C, 52.19; H, 5.24; N, 7.07.

CH_3OOC-Fn-NH-CO-Ala-Ala-OCH_3 (8). Coupling of crude compound **6** (400 mg) in dry methylene chloride with 1.2 mmol of H-Ala-Ala-OCH_3 was performed similarly to the preparation of **4**. TLC purification of the product with CH_2Cl_2/EtOAc (10:1) gave orange crystals (280 mg, 66%) and 110 mg of unreacted carboxazide **5**. Mp: 140–143 °C. IR (KBr): ν 3387, 3357, 3321 (m, NH, assoc.), 1727, 1710 (s, CO_{ester}), 1646 (s, amide I), 1549 (s, amide II) cm^{-1}. FAB-MS: *m*/*z* (%) 459 (100, M^+). Anal. Calcd for $C_{20}H_{25}FeN_3O_6$: C, 52.30; H, 5.49; N, 9.15. Found: C, 52.24; H, 5.48; N, 9.01.

Acknowledgment. We thank the Ministry for Science, Education and Sport of Croatia for support through a grant, the Deutsche Forschungsgemeinschaft for a Heisenberg Fellowship (to K.H.), and the Graduate College "Molecular Probes" for a doctoral scholarship (to D.S.). We are indebted to Ph.D. Leo Frkanec (Rudjer Bošković Institute) for measuring UV/vis and CD spectra.

Supporting Information Available: Gaussian fits of CD spectra of **4**, **7**, and **8**, an ORTEP view of the molecular structure of **8**, crystal packing of compound **8**, the DFT-calculated Cartesian coordinates of all conformers of **7** and **8**, and CD spectra of **4** and **8** in KBr disks. This material is available free of charge via the Internet at http://www.pubs.acs.org.

OM700950R